Eur. Phys. J. Appl. Phys. **35**, 165–172 (2006)
DOI: 10.1051/epjap:2006094

THE EUROPEAN PHYSICAL JOURNAL
APPLIED PHYSICS

Role of hydrogen diffusion on the growth of polymorphous and microcrystalline silicon thin films

A. Fontcuberta i Morral[a] and P. Roca i Cabarrocas

Laboratoire de Physique des Interfaces et des Couches Minces, UMR 7647 CNRS, École Polytechnique, 91128 Palaiseau Cedex, France

Received: 4 October 2005 / Received in final form: 27 December 2005 / Accepted: 6 January 2006
Published online: 2 September 2006 – © EDP Sciences

Abstract. Hydrogen diffusion is monitored during plasma conditions corresponding to the growth of polymorphous and microcrystalline silicon thin films in the temperature range from 50 to 300 °C. Structural changes of the films were monitored in situ by Spectroscopic Ellipsometry measurements and interpreted with the Bruggemann Effective Medium Approximation along with the Tetrahedron Model. For both materials, diffusion of hydrogen leading to the formation of a hydrogen-rich subsurface layer during the first minute of exposure to the hydrogen plasma is observed. This initial phase was followed by a steady-sate regime during which the thickness of the subsurface layer stayed relatively constant and the total film thickness decreased as a function of time. This steady-state is explained as the result of the equilibrium between hydrogen diffusion and etching. The hydrogen diffusion coefficient and etching rate were calculated from these measurements and found to be higher in amorphous than in polymorphous silicon. This result is consistent with the growth dynamics of polymorphous silicon. It also provides information concerning the nucleation of micro-crystallites in amorphous silicon under very large atomic hydrogen flow conditions. Moreover, it also explains why polymorphous silicon films do not undergo the phase transition to microcrystalline, even if deposited under relatively similar large atomic hydrogen flow conditions.

PACS. 61.43.Dq Amorphous semiconductors, metals, and alloys – 66.30.-h Diffusion in solids – 68.55.Ac Nucleation and growth: microscopic aspects

1 Introduction

Atomic hydrogen diffusion is inherent to the growth of silicon thin films by Plasma Enhanced Chemical Vapor Deposition (PECVD). This is due to the fact that the precursors of film growth are obtained by the decomposition of silane (SiH_4) and hydrogen is a natural product of this dissociation. The incorporation of hydrogen in silicon films has the beneficial effect of passivating dangling bonds and restructuring weak bonds [1,2]. Moreover, hydrogen is also involved in the degradation of the electronic properties of amorphous silicon thin films when exposed to light, the Staebler-Wronski effect [3,4]. By increasing the flux of atomic hydrogen towards the films surface with respect to SiH_x radicals during growth, which can be achieved for example by diluting the silane in hydrogen, it is possible to obtain microcrystalline silicon (μc-Si:H). Moreover, under similar dilution conditions but at higher pressure, silicon nanoparticles and clusters are produced in the gas phase and the final material obtained is not microcrystalline but polymorphous silicon (pm-Si:H) [5–7].

It is well established that microcrystalline silicon is a result of a structural transformation of amorphous silicon mediated by hydrogen and therefore that the presence of abundant hydrogen during film deposition is essential for the growth of this material. However, the detailed role of hydrogen in this process is still a subject of debate [8–11].

Hydrogenated polymorphous silicon thin films can also be obtained under high hydrogen dilution, but the difference is that the gas phase chemistry is relatively close to powder formation. Under these conditions, films grow as a result of the incorporation of silicon hydride radicals and ions but also of silicon clusters and nanoparticles of size of 2 to 4 nm and/or agglomerates. The final structure of the material is a relaxed amorphous silicon network with nanocrystalline inclusions [12]. Even if the same amount of atomic hydrogen flow arrives at the surface during deposition of pm-Si:H, these films can be deposited several microns thick without undergoing any phase transformation to μc-Si:H [13]. Consequently, understanding the hydrogen diffusion in amorphous and polymorphous silicon films is important for the understanding of the growth mechanism of μc-Si:H and pm-Si:H.

Several groups have studied the diffusion of hydrogen and determined its diffusion coefficient and activation energy. Most studies are based on ex-situ characterization by Secondary Ion Mass Spectroscopy of thin films that

[a] e-mail: annafm@poly.polytechnique.fr

have been exposed to atomic hydrogen or annealed at various temperatures [14]. In general, ex-situ measurements such as thermally induced hydrogen out-diffusion [15,16] are rather indirect, as it is difficult to relate the data to the growth process and diffusion of hydrogen during growth [17].

Most in situ studies are based on infra red techniques, such the work by Abelson et al. who used ATR technique to study the interaction of thermal atomic hydrogen with a thin amorphous hydrogenated silicon film [18,19]. Such studies were important to determine the positions occupied by H during the diffusion, but could not provide any information on the values of hydrogen diffusion coefficient, due to the fact that infrared absorption was averaged through the whole film. Yamasaki used in situ ESR to deduce information on hydrogen diffusion [20]. However, one should remember that ESR is sensitive to only dangling bonds at the level of 10^{16} cm^{-3}, i.e. orders of magnitude below the density of atomic hydrogen present in the films and diffusing through the sample, meaning that the measurements are sensitive to just a small subset of the diffusing species.

Here we present in situ measurements of the hydrogen diffusion in silicon thin films during their exposure to a hydrogen plasma. The thickness of the hydrogen rich layer is monitored as a function of time by modeling Spectroscopic Ellipsometry measurements with the Tetrahedron model. This experiment is unique and gives a better understanding of the diffusion process, as well as numerical values of the hydrogen diffusion coefficient and its activation energy. The paper is structured as follows. In Section 2 the experimental details are explained. Results are presented in Section 3 and discussed in Section 4. The paper is concluded in Section 5.

2 Experiments

Silicon thin films were deposited by Radio Frequency Plasma Enhanced Chemical Vapor Deposition (RF-PECVD) at 250 °C. Hydrogenated amorphous silicon (a-Si:H) was obtained by the dissociation of pure silane under a total pressure of 6 Pa and RF power of 5 W. For the deposition of polymorphous silicon (pm-Si:H) silane diluted at 2% in hydrogen under a total pressure of 173 Pa and a RF power of 17 W was used. All films were deposited on 1737 Corning glass substrate and had a thickness of 190 nm. Just after deposition (no exposure to air), the films were submitted to a hydrogen plasma under a RF power of 18 W and 133 Pa of pressure at various temperatures in the range of 50 to 300 °C. Spectroscopic Ellipsometry (SE) measurements were done in situ. Both spectroscopic and kinetic measurements were recorded during the hydrogen plasma exposure. Spectroscopic measurements were analyzed by a combination of the Tetrahedron model and the Bruggemann Effective Medium Approximation, giving structural information of the film such as thickness and variations in the hydrogen content [21]. Kinetic measurements at a photon energy of 3.55 eV (highly sensitive to the film surface) were used to understand the dynamics of the hydrogen diffusion.

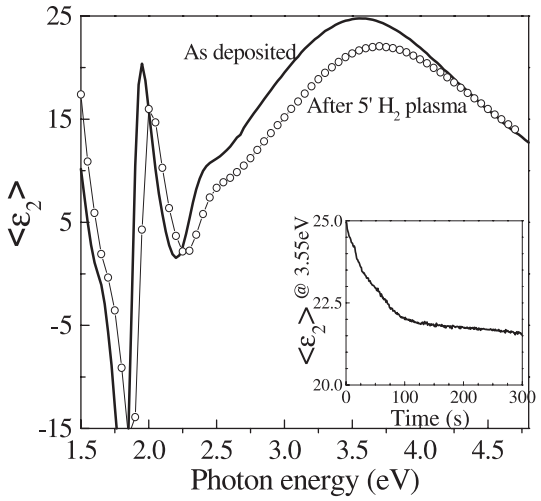

Fig. 1. Imaginary part of the pseudo-dielectric function of a ∼0.2 μm of a-Si:H thin film, as deposited and after 5 min of hydrogen plasma at 250 °C. The inset shows the evolution of $\langle\varepsilon_2\rangle$ at a photon energy of 3.55 eV.

3 Results

3.1 In situ measurement of hydrogen diffusion coefficient and etching rate

Figure 1 shows the imaginary part of the pseudo-dielectric function $\langle\varepsilon_2\rangle$ measured by SE on a 1927 Å thick a-Si:H film before and after 5 min of hydrogen plasma exposure. The as-deposited spectrum is characteristic of a-Si:H, with a broad band centered at 3.55 eV. The interference fringes in the lower energy part of the spectrum give information on the film thickness. Information on the dielectric function of the material and the surface roughness is given by the high energy part of the spectrum. After 5 min of hydrogen plasma, the interference fringes have slightly shifted to higher energies due to a slight decrease of the total thickness. The central broad band has shifted also to higher energies and decreased in amplitude. As shown below, this is due to the formation of a hydrogen-rich sub-surface layer. Spectra in Figure 1 were analyzed with a combination of the Tetrahedron model and the Bruggemann Effective Medium Approximation. From this analysis, it is possible to quantify the increase in hydrogen content of the film [21]. The results of the analysis of the SE measurements of Figure 1 are shown in Table 1. After 5 min, hydrogen plasma has etched away a total thickness of 84 Å and formed a hydrogen rich sub-surface layer with thickness $\Delta d_{\mathrm{H}} = 246$ Å. The hydrogen concentration in this layer has increased from 8% (typical of a-Si:H deposited at 250 °C) to 23%, and the void fraction has increased by 5%. The hydrogen concentration measured with this method corresponds to bound hydrogen, as further evidenced by previous Infrared Spectroscopy studies [22,23].

Table 1. Composition of a a-Si:H thin film after deposition and after a 5 min exposure to a hydrogen plasma, deduced by the analysis of the Spectroscopic Ellipsometry data represented in Figure 1.

Type of sample	Total thickness Å	Surface Roughness Å	Bulk layer Å	Bulk layer %void	Bulk layer %H	Sub-surface layer Å	Sub-surface layer %void	Sub-surface layer %H
As deposited	1927	15	1912	1	8	–	–	–
After 5' H_2 plasma	1843	14	1583	1	8	246	5	23

In these studies it was also shown the different configurations that hydrogen adopts during this process. This is however outside the outlook of this paper. The inset in Figure 1 shows the kinetic evolution of $\langle\varepsilon_2\rangle$ at 3.55 eV during the first 5 min of hydrogen plasma. (At this photon energy $\langle\varepsilon_2\rangle$ is highly sensitive to the film surface). As shown in the figure, the decrease of $\langle\varepsilon_2\rangle$, related to the formation of the hydrogenated layer, occurs mainly in the first minute of hydrogen plasma exposure. As shown in the following, a hydrogen-rich layer is formed during the initial stages of the plasma. Once the hydrogen rich layer is formed, the etching rate increases very rapidly. Then, etching and hydrogen come into equilibrium. As it will be proven, the thickness of the hydrogenated layer remains than constant as a consequence of this equilibrium. This is why the amplitude of $\langle\varepsilon_2\rangle$ remains also constant after the equilibrium between etching and diffusion is achieved.

In order to study more accurately the formation of the hydrogen rich sub-surface layer, SE measurements were recorded with a period of 10 seconds during the first 120 s of plasma exposure at 250 °C. From the spectra, Δd_{H} could be deduced. Figure 2a shows the evolution of the thickness of the hydrogenated layer as well as the thickness of the whole film. We can see that the hydrogenated subsurface layer forms in the first minute of hydrogen plasma exposure, and that during this period the total film thickness remains practically constant. Once the hydrogen-rich subsurface layer has been formed, its thickness Δd_{H} remains constant and the total film thickness starts to linearly decrease as a function of time, yielding an etching rate of 0.52 Å/s. This analysis indicates that etching requires the formation of a highly hydrogenated layer, and thus during the initial stages of hydrogen exposure diffusion dominates over etching. This is further supported by the inset in Figure 2a, where the thickness of the subsurface layer is plotted as a function of $\sqrt{t}$. The relation between Δd_{H} and $\sqrt{t}$ in the early stages of hydrogen plasma is linear and the slope yields the diffusion coefficient of hydrogen, D_{H}. At 250 °C, we obtained a value of D_{H} of 8×10^{-14} cm^2/s, in agreement with a previous work, in which we have already used this technique to monitor the hydrogen diffusion in a-Si:H [24,25]. We would like to add that hydrogen concentration and profiles deduced from the SE data have been previously checked against Secondary Ion Mass Spectroscopy measurements [20]. The same procedure applied to study hydrogen diffusion in pm-Si:H yielded a diffusion coefficient of 1.3×10^{-14} cm^2/s at 250 °C, i.e., almost one order of magnitude smaller

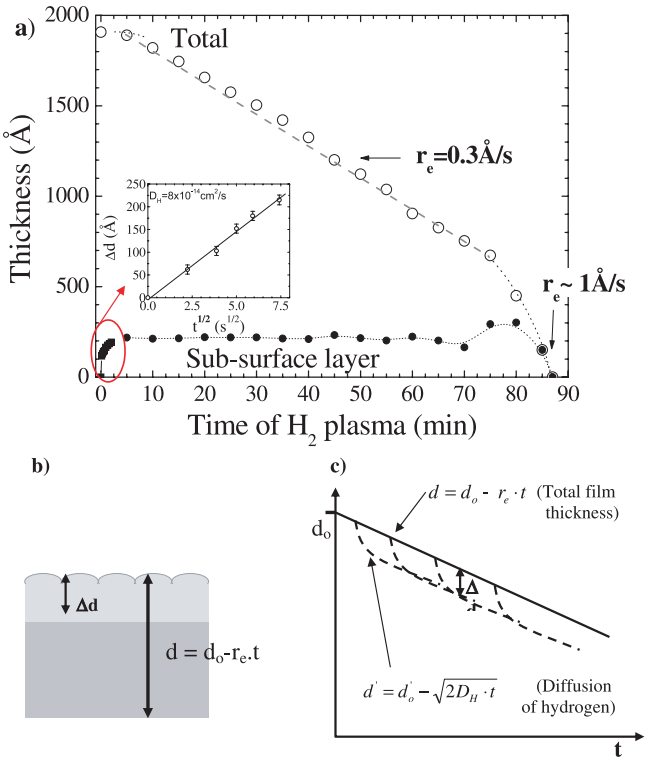

Fig. 2. (a) Evolution of the thickness of the whole film and the sub-surface layer of an a-Si:H film exposed to a hydrogen plasma at 250 °C. Note the initial delay in etching due to the formation of the sub-surface layer. In the inset thickness evolution of the hydrogenated sub-surface layer as a function of the square root of time. The hydrogen diffusion coefficient is obtained from the initial slope. (b) Schematics of the diffusion and etching of the silicon layer by the hydrogen plasma. (d_o is the initial thickness, r_e the etching rate and Δd the thickness of the hydrogenated sub-surface layer).

than that of a-Si:H, but one order of magnitude higher than the value $D_{\mathrm{H}} = 7 \times 10^{-16}$ cm^2/s for crystalline silicon [26]. Concerning the etching rates, the values obtained are 0.52 Å/s for a-Si:H and 0.42 Å/s for pm-Si:H.

Considering the equilibrium between hydrogen diffusion and hydrogen etching (see Fig. 2), it is possible to relate the etching rate r_e, D_{H} and Δd_{H}. Considering that the film thickness decreases at an etch rate r_e and that the hydrogen front progresses as $\sqrt{2D \cdot t}$, the equilibrium

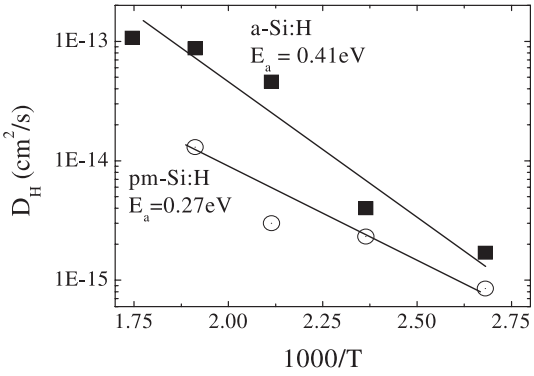

Fig. 3. Temperature dependence of the diffusion coefficient of hydrogen in a-Si:H and pm-Si:H films deposited at 250 °C. The activation energy is proportional to the value of the slope.

thickness of the hydrogenated layer, Δd_{H}, should be:

$$\Delta d_{\mathrm{H}} = \frac{D}{2 \cdot r_e} \tag{1}$$

which is satisfied by all the values of D_{H} and r_e obtained. It is important to notice that the decrease of $\langle \varepsilon_2 \rangle$ at 3.55 eV during the initial plasma exposure corresponds to the formation of the hydrogenated layer. Therefore, monitoring the kinetic evolution of $\langle \varepsilon_2 \rangle$ at 3.55 eV (Fig. 1) is directly related to the characteristic time of formation (τ) of the hydrogenated layer and will be used for the discussion in Sections 4.2 and 4.3.

3.2 Temperature dependence of diffusion and etching in a-Si:H and pm-Si:H thin films

The effect of hydrogen plasma at various temperatures on a-Si:H and pm-Si:H films deposited at 250 °C was studied following the same procedure as described above. From SE measurements we deduced the temperature dependence for H diffusion and etching processes in the two types of films. Hydrogen diffusion followed the Arrhenius law:

$$D_{\mathrm{H}} = D_o \exp \frac{-E_a^D}{K_B T} \tag{2}$$

where K_B is the Boltzmann constant, T the temperature, E_a^D the activation energy of hydrogen diffusion, and D_o the diffusion prefactor. D_{H} in a-Si:H and pm-Si:H are plotted semi-logarithmically versus $1000/T$ in Figure 3. The 'apparent' activation energy of diffusion was calculated from the slope. The values of E_a and D_o are given in Table 2. They are both higher for a-Si:H than for pm-Si:H ($E_a = 0.41$ eV, $D_o = 1.75 \times 10^{-8}$ cm^2/s versus $E_a = 0.27$ eV, $D_o = 1.25 \times 10^{-10}$ cm^2/s). The values of E_a and D_o obtained are in agreement with the Meyer-Neldel relation (NMR), which describes the relation between E_a and D_o over 8 orders of magnitude [27–29].

The etching rate of a-Si:H and pm-Si:H, measured at different temperatures, also followed an Arrhenius behavior, with a negative activation energy E_a^e:

$$r_e = r_{eo} \exp \frac{-E_a^e}{K_B T} \tag{3}$$

Table 2. Values of the activation energy and the diffusion coefficient prefactor, obtained by the temperature dependence of the hydrogen diffusion coefficient.

Material	E_a (eV)	D_o (cm^2/s)
a-Si:H	0.41	1.75×10^{-8}
pm-Si:H	0.27	1.25×10^{-10}
c-Si	–	$\ll 1 \times 10^{-14}$

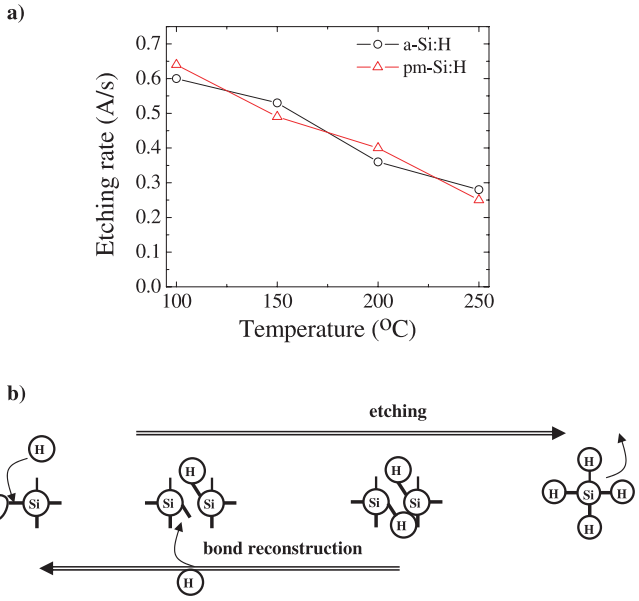

Fig. 4. (a) Etching rate as a function of the inverse temperature. (b) Schematics of the bond breaking reactions that take place during hydrogen etching. The reverse reaction of bond rearrangement and reconstruction is also schematized.

here r_{eo} is the r_{eo} the etching rate prefactor. The etching rate for a-Si:H and pm-Si:H are plotted in Figure 4a. The etching rate and therefore also activation energy for etching of pm-Si:H and a-Si:H are very similar respectively –42 meV and –37 meV. They are an order of magnitude smaller than the activation energy for diffusion, which can be taken as an indication for hydrogen diffusion, or rather the formation of the hydrogen-rich and porous subsurface layer, being the rate limiting step for the etching. This is supported by the fact that the etching rate is multiplied by a factor of 4 during the last minute of etching as shown in Figure 2a, i.e. when the hydrogen accumulates at the interface with the glass substrate. A discussion of the relation of these results with the structure of a-Si:H and pm-Si:H is presented in the following section.

4 Discussion

In this section, we first discuss the results on hydrogen diffusion and etching in relation to the structure of a-Si:H and pm-Si:H. Then, the implications on the growth models of amorphous, polymorphous and microcrystalline silicon are highlighted.

4.1 Influence of the structural properties of a-Si:H and pm-Si:H on hydrogen diffusion and etching

Polymorphous silicon is a nanostructured material with an improved medium range order and electronic properties with respect to a-Si:H [30]. It consists of a dense silicon network with embedded nanocrystals, as a consequence of being deposited under conditions close to powder formation, where hydrogenated silicon radicals, clusters and nanocrystals contribute to the film growth [31,32].

Diffusion of hydrogen in a-Si:H proceeds mainly through a combination of bond breaking and insertion of H in weak or dangling bonds. The diffusion coefficient of hydrogen in pm-Si:H is one order of magnitude lower than in a-Si:H, and one higher than crystalline silicon, c-Si [33]. This is not surprising, since the matrix of pm-Si:H is more relaxed and its defect density is one order of magnitude lower than in a-Si:H [34,35]. It is consistent with pm-Si:H being a material with structural properties intermediate between those of a-Si:H and c-Si.

Hydrogen etching proceeds through multiple hydrogen insertion steps in the silicon network. Hydrogen insertion occurs by breaking a Si-Si bond. Each step is reversible, meaning that the broken Si-Si bonds can reconstruct, with the consequent desorption of atomic or molecular hydrogen and/or silane [36]. This mechanism is schematized in Figure 4b. The activation energy has to be necessarily negative because etching corresponds to the reverse reaction of bond reconstruction, which has positive activation energy. A negative energy has already been measured in this range of temperatures for gaseous silicon etching [37].

The activation energy for etching of pm-Si:H is –42 meV and –37 meV for a-Si:H. One could think that this energy is rather low, especially when compared with the activation energy of hydrogen diffusion. One can understand that the energy barrier for bond breaking and reconstruction is lower for a highly porous and hydrogenated material than in a dense one, deriving in a much smaller activation energy. As shown in Figure 4, a-Si:H is etched at a very similar rate as pm-Si:H in all the range of temperatures measured. However, the activation energy deduced from the slope is 37 meV for a-Si:H and 42 meV for pm-Si:H. It is slightly higher in the case of pm-Si:H, in agreement with the picture that the Si-Si bonds in this material are more stable.

In Figure 5a, b the time required for the formation of the sub-surface hydrogenated and porous layer (τ) and the steady-state thickness of this layer (Δd_{H}) are plotted as functions of the temperature for a-Si:H and pm-Si:H. For example, at a substrate temperature of 100 °C, it takes 18 s to form a 150 Å thick hydrogenated sub-surface layer in a-Si:H, whereas in the case of pm-Si:H it takes 35 s to form a significantly thinner layer (110 Å). At higher substrate temperatures, the values of τ and Δd_{H} increase for both a-Si:H and pm-Si:H, in accordance with equation (1) and with a much more pronounced increase of hydrogen diffusion than a decrease of etching. In summary, there are two consequences of the slower diffusion of hydrogen in pm-Si:H, which are that the formation of a sub-surface hydrogen-rich layer occurs more slowly and that the thickness of the layer is also smaller.

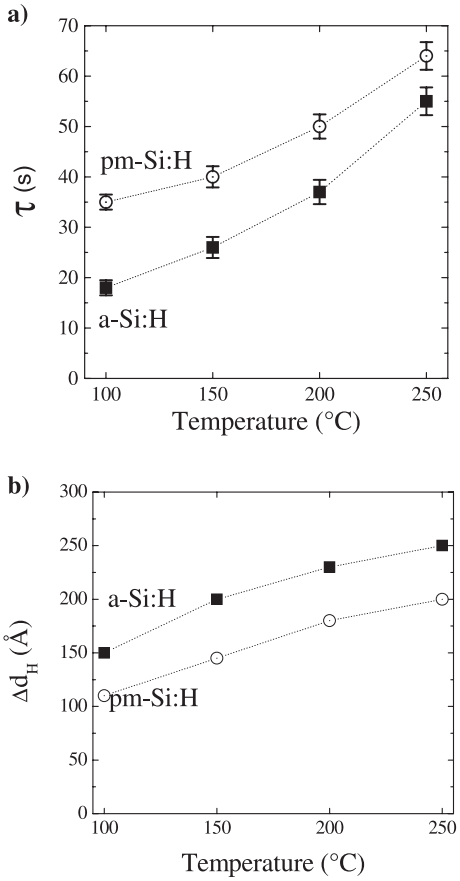

Fig. 5. (a) τ, the characteristic time of formation of the hydrogen-rich sub-surface layer and (b) Δd_{H}, the thickness of the hydrogen-rich sub-surface layer as a function of temperature for a-Si:H and pm-Si:H.

4.2 Consequences on the growth models of polymorphous and microcrystalline silicon films

Polymorphous and microcrystalline silicon films are obtained by PECVD under conditions where there is a large flux of atomic hydrogen during film deposition. The only deposition parameter that changes between the two is the total gas pressure. Deposition at higher gas pressures results in the formation of clusters and nanoparticles in the gas phase, which contribute to the growth of the film [32]. Contrary to μc-Si:H and protocrystalline silicon [38], pm-Si:H thin films can be grown as thick as several microns without changing their structural characteristics. Microcrystalline silicon is the result of transformation of a-Si:H mediated by a very fast diffusion of hydrogen. a-Si:H is first transformed into an intermediate porous and highly hydrogenated phase, which constitutes the phase where the crystallites nucleate. Once nucleated, crystallites grow forming a crystalline and much denser film [39].

We have shown in previous work that pm-Si:H has different growth kinetics due to the contribution of clusters

and nanoparticles. Clusters and nanoparticles produced in the gas phase prior deposition can be pushed to the substrate by the gas drag or by the presence of a large enough force towards the substrate. On the contrary, if the thermophoretic force is applied out of the substrate, it is possible to deposit a film without clusters and nanoparticles. This can be achieved by applying a positive temperature gradient between the electrodes (meaning that the RF electrode is colder). We have shown that at thermal gradients higher than 50 ° C/cm, the thermophoretic force is larger than gas drag and the nanoparticles and clusters are pushed away from the substrate. The resultant material grown under those conditions where the nanoparticles are not deposited is not pm-Si:H. The growth dynamics is very similar to those of μc-Si:H, meaning that the film is initially amorphous and is successively transformed into hydrogenated and porous until the first crystallites appear and μc-Si:H is formed [40]. This result shows that the contribution of clusters to the deposition had an effect on the formation of the hydrogenated layer where crystallites nucleate. However, this study did not address the question of why the absence of clusters and nanoparticles to the deposition would suppress the transformation of the thin film into a porous and highly hydrogenated layer necessary for the nucleation of microcrystalline silicon.

During PECVD deposition of silicon thin films there is always a flux of atomic hydrogen to the surface. This flux is especially relevant under high hydrogen dilution conditions, such as the ones used for the deposition of polymorphous and microcrystalline silicon. This means that during deposition, the flow of silicon based radicals contributing to the increase of the total thickness coexists with the diffusion of atomic hydrogen through the layer. In deposition conditions in which the flux of atomic hydrogen is comparable to the flux of silicon based radicals, silicon thin films should become porous and highly hydrogenated. Assuming a reasonable deposition rate and with the results of this study on hydrogen diffusion, it is possible to evaluate if hydrogen diffusion is large enough to transform a film into a porous and hydrogenated layer during growth. We have used the obtained values of D_{H} and typical deposition rates to understand the difference of film evolution during polymorphous and microcrystalline silicon growth. We illustrate the processes of hydrogen diffusion and increase of the film thickness in Figure 6. The thickness of a film as a function of time is indicated by the continuous line, in the case of a typical deposition rate of 2 Å/s. To illustrate the diffusion of hydrogen occurring during deposition, the progression of hydrogen through a-Si:H and pm-Si:H at different times is indicated by dashed lines. For this purpose we have used a time dependence of the form $\sqrt{2D_{\mathrm{H}} \cdot t}$ and the values of D_{H} of a-Si:H and pm-Si:H at 250 °C (see Tab. 2). While the whole process is certainly more complex (besides deposition and diffusion one should also consider etching, porous layer formation, UV light effects, ...), we think that this simplified picture illustrates some important features. In Figure 6, the dark line represents the increase of layer thickness due to the deposition process and the dashed line the progression of hydrogen through the deposited layer. There are two kinds of dashed lines, the darker ones for pm-Si:H and the lighter ones for a-Si:H. With this graph, we intend to show the difference in the hydrogenation process of the two kinds of films occurring during deposition. For example in point A, after 150 s of deposition, all the atomic hydrogen impinging on the surface of the a-Si:H during the first 110 s has diffused up to the interface with the substrate (see point A_2). The amount of hydrogen in the case of pm-Si:H, is reduced to more than a half; only the atomic hydrogen impinging the surface during the first 50 s has diffused down to the interface with the substrate (B, A_1). Thus polymorphous silicon films do not undergo the transition to microcrystalline silicon because of the slow diffusion of hydrogen.

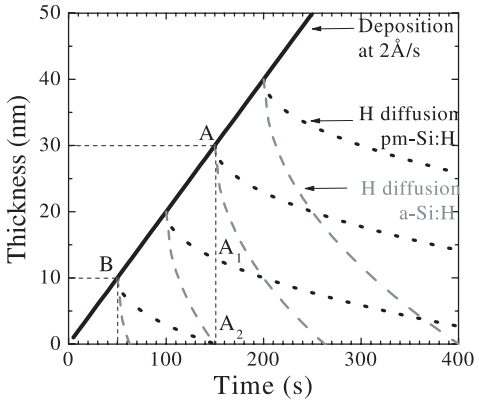

Fig. 6. Progress of the atomic hydrogen diffusing fronts thorough the growing surface, calculated with the D_{H} of a-Si:H and pm-Si:H.

As a consequence of the large concentration of atomic hydrogen in the gas phase during pm-Si:H deposition, one should expect that the hydrogen content of pm-Si:H films to be higher to the hydrogen content of standard a-Si:H. This is indeed the case: pm-Si:H is a dense material that can have hydrogen contents up to 20% while retaining a high density [41].

4.3 Nucleation of μc-Si:H

The kinetics of formation of the hydrogenated sub-surface layer and the relation with the nucleation and growth of μc-Si:H are discussed in this section. μc-Si:H is usually obtained by plasma enhanced decomposition of silane, mixed with a very large proportion of hydrogen. A second method of depositing μc-Si:H is the Layer-by-Layer method (LBL), which consists on the alternation of a deposition of a-Si:H during a time T_{Si} and a hydrogen plasma during a time T_{H}. The advantage of this technique, is that it makes possible to distinguish the effect of hydrogen on the nucleation of μc-Si:H from all the complex chemistry of a mixed hydrogen and silane plasma. At low values of the ratio $T_{\mathrm{H}}/T_{\mathrm{Si}}$ the material obtained is just a porous a-Si:H. By increasing the ratio μc-Si:H is obtained. At the extreme of very large ratios the hydrogen plasma completely etches the film deposited during T_{Si} and no film is

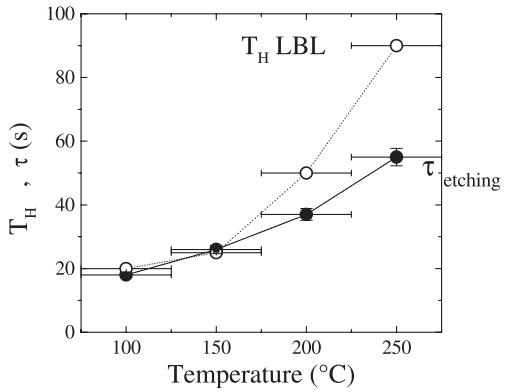

Fig. 7. Comparison of the characteristic time of formation of the hydrogenated sub-surface layer, τ, to the T_{H} used in LBL for the deposition of μc-Si:H on a pre-existing a-Si:H thin film at different temperatures. For a more appropriate comparison with the LBL process, the a-Si:H thin film was deposited and exposed to a hydrogen plasma at the same temperature.

obtained. In situ investigations of the deposition of μc-Si:H by LBL along with TEM measurements showed that crystallites nucleate and grow in a low density layer. It was proposed that the low density layer was formed by the diffusion of hydrogen during T_{Si} [42,43]. Some correlations with the values of D_{H} found in the literature were done, but there was never a direct correlation with an in situ measurement of diffusion of hydrogen. Another experimental observation was that the value of T_{H} for the obtaining of an equivalent μc-Si:H had to be decreased at lower temperatures [44]. The reason of that was not clear. The hypotheses about the necessity to decrease T_{H} at lower temperatures were related to: (1) the increase of the etching rate, (2) to the decrease of hydrogen diffusion at lower temperatures, or (3) to the increase of atomic hydrogen flux due to a lower recombination on the deposition chamber walls... However, Optical Spectroscopy Measurements of the hydrogen plasma at different temperatures showed that the atomic hydrogen concentration does not depend on the substrate temperature [13]. Therefore, the last hypothesis had to be ruled out.

In Figure 7 the characteristic time of formation of the hydrogenated sub-surface layer, τ, is compared to the T_{H} used for the deposition of μc-Si:H on a pre-existing a-Si:H thin film at different temperatures. For a more appropriate comparison with the LBL process, the a-Si:H thin film was deposited and exposed to a hydrogen plasma at the same temperature. T_{H} corresponds to the time necessary for the obtaining of a crystalline fraction of 60%. The value of T_{H} is 20 s for a deposition temperature of 100 °C and increases in an exponential way up to 90 s at 250 °C. The values of τ follow the same trend within the error bars. In Figure 5b, Δd_{H}, the thickness of the hydrogenated sub-surface layer formed during the hydrogen plasma exposure during τ is represented as a function of temperature. Δd_{H}, which is a result of the equilibrium between diffusion and etching by hydrogen, increases with temperature from 120 Å at 100 °C to 280 Å at 250 °C. The increase of Δd_{H}, which follows equation (1), can be explained by the increase of D_{H} by one order of magnitude from 100 to 250 °C, but in any case it cannot be explained to a decrease by the etching rate, which is only of 20%. In conclusion, from the three initial hypotheses only the decrease of D_{H} can explain the change of T_{H} as a function of temperature.

5 Conclusions

Amorphous and polymorphous silicon have been exposed to a hydrogen plasma at different temperatures. Hydrogen diffusion and etching have been monitored in situ by Spectroscopic Ellipsometry and the diffusion coefficient, the etching rate and their temperature dependence have been obtained. The diffusion coefficient of hydrogen in pm-Si:H is about one order of magnitude lower than in a-Si:H. D_{H} is thermally activated for both materials, with an activation energy of 0.41 eV for a-Si:H and 0.27 eV for pm-Si:H. The etching rate of pm-Si:H is about 10% lower. The low values of D_{H} of pm-Si:H were associated to its heterogeneous structure with respect to a-Si:H. Moreover, a lower value of D_{H} also explains why pm-Si:H does not undergo the same hydrogen-induced phase transition which transforms a-Si:H into μc-Si:H, even if it is deposited under conditions of high atomic hydrogen flux. Finally, it is shown that the hydrogen dilution dependence of the nucleation of μc-Si:H at different temperatures is explained by the change in hydrogen diffusion and not etching.

References

1. C. Mandfredotti, F. Fizzotti, M. Boero, P. Pastorino, P. Polesello, E. Vittone, Phys. Rev. B **50**, 18046 (1994)
2. Z. Remeš, M. Vaněček, A.H. Mahan, R.S. Crandall, Phys. Rev. B **56**, R12710 (1997)
3. D.L. Staebler, C.R. Wronski, Appl. Phys. Lett. **31**, 292 (1977)
4. H.M. Branz, Phys. Rev. B **59**, 5498 (1999)
5. Vepřek, V. Mareček, Solid State Electron. **11**, 683 (1968)
6. P. Roca i Cabarrocas, A. Fontcuberta i Morral, B. Kalache, S. Kasouit, Solid State Phenom. **93**, 257 (2003)
7. S. Lebib, P. Roca i Cabarrocas, Eur. Phys. J. Appl. Phys. **26**, 17 (2004)
8. I. Kaiser, N.H. Nickel, W. Fuhs, W. Pilz, Phys. Rev. B **58**, R1718 (1998)
9. K. Nomoto, Y. Urano, J.L. Guizot, G. Ganguly, A. Matsuda, Jpn J. Appl. Phys. **29**, L1372 (1990)
10. S. Sriraman, S. Agarwal, E.S. Aydil, D. Maroudas, Nature **418**, 62 (2002)
11. N. Layadi, P. Roca i Cabarrocas, B. Drévillon, I. Solomon, Phys. Rev. B **52**, 5136 (1995)
12. A. Fontcuberta i Morral, H. Hofmeister, P. Roca i Cabarrocas, J. Non-Cryst. Solids **299–302**, 284 (2002)
13. A. Fontcuberta i Morral, Ph.D. Thesis, École Polytechnique, Palaiseau, France, 2001, Chap. 4
14. W. Beyer, U. Zastrow, J. Non-Cryst. Solids **227–230**, 880 (1998)
15. W. Beyer, H. Wagner, J. Non-Cryst. Solids **59, 60**, 161 (1983)

16. Yu.L. Khait, R. Weil, R. Beserman, W. Beyer, H. Wagner, Phys. Rev. B **42**, 9000 (1990)
17. R.A. Street, Phys. Rev. B **53**, 2454 (1991)
18. A. von Keudell, J.R. Abelson, J. Appl. Phys. **84**, 489 (1998)
19. M. Katiyar, J.R. Abelson, Mat. Sci. Eng. A **304**, 349 (2001)
20. U.K. Das, T. Yasuda, S. Yamasaki, Phys. Rev. Lett. **85**, 2324 (2000)
21. A. Fontcuberta i Morral, P. Roca i Cabarrocas, C. Clerc, Phys. Rev. B **69**, 125307 (2004)
22. S. Vignoli, A. Fontcuberta i Morral, R. Butte, R. Meaudre, M. Meaudre, J. Non-Cryst. Solids **299–302**, 220 (2002)
23. S. Vignoli, P. Melinon, B. Masenelli, P. Roca i Cabarrocas, A.M. Flank, C. Longeaud, J. Phys.-Condens. Mat. **17**, 1279 (2005)
24. A. Fontcuberta i Morral, P. Roca i Cabarrocas, J. Non-Cryst. Solids **299–302**, 196 (2002)
25. F. Kail, A. Fontcuberta i Morral, A. Hadjadj, P. Roca i Cabarrocas, A. Beorchia, Philos. Mag. B1 **84**, 595 (2004)
26. H.C. Neitzert, N. Layadi, P. Roca i Cabarrocas, R. Vanderhagen, M. Kunst, J. Appl. Phys. **78**, 1438 (1995)
27. W.B. Jackson, Phys. Rev. B **38**, 3595 (1988)
28. J. Shinar, R. Shinar, X.-L. Wu, S. Mitra, R.F. Girvan, Phys. Rev. B **43**, 1631 (1991)
29. W. Beyer, Mat. Res. Soc. Symp. Proc. **664** (2001)
30. R. Meaudre, R. Butte, S. Vignoli, M. Meaudre, L. Saviot, O. Marty, P. Roca i Cabarrocas, Eur. Phys. J. Appl. Phys. **22**, 171 (2003)
31. P. Roca i Cabarrocas, S. Hamma, S.N. Sharma, G. Viera, E. Bertran, J. Costa, J. Non-Cryst. Solids **227–230**, 871 (1998)
32. A. Fontcuberta i Morral, H. Hofmeister, P. Roca i Cabarrocas, J. Non-Cryst. Solids **299–302**, 284 (2002)
33. K.J. Chang, D.J. Chadi, Phys. Rev. B **40**, 11644 (1989)
34. S. Vignoli, P. Mélinon, B. Masenelli, P. Roca i Cabarrocas, A.M. Flank (submitted to Phys. Rev. Lett.)
35. M. Meaudre, R. Meaudre, R. Butte, S. Vignoli, C. Longeaud, J.P. Kleider, P. Roca i Cabarrocas, J. Appl. Phys. **86**, 946 (1999)
36. K. Sasaki, H. Tomoda, T. Takada, Vacuum **51**, 537 (1998)
37. D.E. Ibbotson, J.A. Mucha, D.L. Flamm, J.M. Cook, J. Appl. Phys. **56**, 2939 (1984)
38. J.M. Pearce, R.J. Koval, A.S. Ferlauto, R.W. Collins, C.R. Wronski, Appl. Phys. Lett. **77**, 3093 (2000)
39. A. Fontcuberta i Morral, J. Bertomeu, P. Roca i Cabarrocas, Mat. Sci. Eng. B **69, 70**, 559 (2000)
40. A. Fontcuberta i Morral, P. Roca i Cabarrocas, Thin Solid Films **383**, 161 (2001)
41. R. Meaudre, R. Butte, S. Vignoli, M. Meaudre, L. Saviot, O. Marty, P. Roca i Cabarrocas, Eur. Phys. J. Appl. Phys. **22**, 171 (2003)
42. C. Godet, N. Layadi, P. Roca i Cabarrocas, Appl. Phys. Lett. **66**, 3146 (1995)
43. A. Fontcuberta i Morral, J. Bertomeu, P. Roca i Cabarrocas, Mat. Sci. Eng. B **69, 70**, 559 (2000)
44. S. Hamma, Ph.D. Thesis, University Paris VI, 1998, p. 87